# CHARACTERIZATION OF MICROBIAL SIDEROPHORES BY MASS SPECTROMETRY

**Tomáš Pluháček,[1,2] Karel Lemr,[1,2] Dipankar Ghosh,[3] David Milde,[1] Jiří Novák,[2] and Vladimír Havlíček[1,2]***

[1]*Department of Analytical Chemistry, Faculty of Science, Regional Centre of Advanced Technologies and Materials, Palacky University, 17. listopadu 12, 771 46, Olomouc, Czech Republic*
[2]*Institute of Microbiology, AS CR v.v.i., Videnska 1083, CZ 142 20, Prague 4, Czech Republic*
[3]*Special Centre for Molecular Medicine, Jawaharlal Nehru University, New Delhi 110067, India*

*Received 1 July 2014; accepted 19 December 2014*

*Published online in Wiley Online Library (wileyonlinelibrary.com). DOI 10.1002/mas.21461*

*Siderophores play important roles in microbial iron piracy, and are applied as infectious disease biomarkers and novel pharmaceutical drugs. Inductively coupled plasma and molecular mass spectrometry (ICP-MS) combined with high resolution separations allow characterization of siderophores in complex samples taking advantages of mass defect data filtering, tandem mass spectrometry, and iron-containing compound quantitation. The enrichment approaches used in siderophore analysis and current ICP-MS technologies are reviewed. The recent tools for fast dereplication of secondary metabolites and their databases are reported. This review on siderophores is concluded with their recent medical, biochemical, geochemical, and agricultural applications in mass spectrometry context.* © 2015 Wiley Periodicals, Inc. Mass Spec Rev.

**Keywords:** *iron; siderophores; mass spectrometry; biomarkers; dereplication*

## I. INTRODUCTION

This review is dedicated to mass spectrometry analysis of microbial siderophores, important natural iron chelators. Iron is a highly vital essential nutrient both in microbes and mammals. Consequently, competition for iron is often a conserved feature in most host-pathogen interactions (Haas, 2012). Not surprisingly, both microbes and mammals have evolved numerous strategies for iron fitness. Mammals have learnt to always limit availability of free iron and instead conceal this element in complexes with iron binding proteins such as transferrin, lactoferrin, ferritin, and others, or incorporate iron into compounds such as heme in haemoglobin (Morgenthau, Beddek, & Schryvers, 2014). In order to overcome limited bioavailability of free iron in their hosts, pathogens have evolved many different energy-dependent iron acquisition systems from mammalian complexes. One class of iron acquisition systems is represented by siderophores, secretory low-molecular-weight iron-chelating compounds, used by microbes to scavenge iron from host iron-binding proteins (Haas, Eisendle, & Turgeon, 2008). Subse-). Subsequently, the iron-siderophore complexes are transported into the microbes via specific receptors on the microbial cell surface and the iron is released. The ligating groups contain mostly oxygen atoms (of hydroxamate, catecholate, α-hydroxy- and α-keto-carboxylic acids) as well as nitrogen atoms. The latter case is represented e.g., by maduraferrin, in which iron binding nitrogen of hexahydropyridazine-3-carboxylic acid is negatively charged (Kellerschierlein et al., 1988). On the other hand, microbial biosynthetic machinery also involves diverse products including crystalline metal nanoparticles (Siponen et al., 2013). Recently, transferring bacterial magnetosome gene clusters to easily handled microorganisms enabled synthetic production of monodisperse single magnetic domain nanoparticles at ambient temperature (Kolinko et al., 2014). In addition to ferromagnetic $Fe_3O_4$ or $Fe_3S_4$ nanoparticles, some bacteria yeasts and fungi produce gold, ZnS, CdS, zirconium, and silver nanoparticles (Asmathunisha & Kathiresan, 2013). Metal nanoparticle producers can also be found among important human fungal pathogens (Bhainsa & D'Souza, 2006). Therefore, extracellular scavenging and acquisition of essential elements using energy dependent protein complexes is an evolutionary conserved fitness factor for all pathogens and consequent target for potential therapeutic strategies.

In addition to biochemical applications, siderophores enjoy considerable potential in biotechnology and pharmaceutical sector. The obligator significance of siderophores in pathogens may allow using siderophores as *Trojan horses*, representing a novel class of antibiotics with considerable therapeutic potential (Bassetti et al., 2013; Fernandes & de Carvalho, 2014; Miller et al., 2009). Growing pool of evidence indicates that siderophores and their semisynthetic analogues may be used in anti-cancer therapeutic strategies (Brard, Granai, & Swamy, 2006; Keeler & Brookes, 2013). Siderophores have also been demonstrated to enjoy potential in magnetic resonance imaging (MRI) (Ding, Helquist, & Miller, 2008) or positron emission tomography reagents (Petrik et al., 2010). Microbial siderophores can also be used as specific disease biomarkers in cases when ribosomal protein fingerprinting is difficult (Bertrand

Contract grant sponsor: Ministry of Education, Youth and Sports of the Czech Republic; Contract grant number: LD13038; Contract grant sponsor: Czech Science Foundation; Contract grant number: P206/12/1150.

*Correspondence to: Vladimír Havlíček, Institute of Microbiology, AS CR v.v.i., Videnska 1083 CZ 142 20, Prague 4, Czech Republic. E-mail: vlhavlic@biomed.cas.cz

et al., 2009; Ye et al., 2013). They also have wide applications in bioremediation (Dimkpa et al., 2009a) and geochemistry (Duckworth et al., 2009). Biocontrol involving plant-pathogenic fungi interaction is another fascinating application area of siderophores (Tortora, Diaz-Ricci, & Pedraza, 2011).

The analysis of siderophores in natural samples (seawater, soil, biological fluids) presents many unique challenges. In natural samples, siderophores are often present in low concentrations and exist in multi-protein complexes. In order to address concentration issues, most analytical strategies for siderophores usually employ pre-concentration of samples by solid phase extraction (SPE) with columns packed with reversed-phase or ion-exchange sorbents and subsequently isolated by high performance liquid chromatography (HPLC). In nuclear magnetic resonance (NMR) spectroscopy characterization, the metal is generally removed from the complex prior to data acquisition, as $Fe^{3+}$ causes line broadening of NMR signals (Birus et al., 1995). To obtain NMR spectra of siderophores in metal-chelated form, usually the diamagnetic $Ga^{3+}$ or $Al^{3+}$ siderophore analogs are employed. In this review we summarize enrichment procedures and mass spectrometry armory capable to trace siderophores and characterize their structure. The critical evaluation is focused to mass data filtering, isotopic structure and iron localization using separations followed by mass spectrometry.

## II. CHARACTERISTICS OF MICROBIAL SIDEROPHORES

Siderophores involve hydroxamate, catecholate, phenolate, α-hydroxycarboxylate, or mixed-function groups capable to form coordination complexes with very high affinity and selectivity for ferric ions (Hider & Kong, 2010). The biosynthesis of microbial secondary metabolites is manifested through sophisticated molecular machinery involving diverse ribosomal, hybrid, or non-ribosomal polyketide synthases (NRPS) (Franke, Ishida, & Hertweck, 2014; Kalb, Lackner, & Hoffmeister, 2013). Siderophores are mostly biosynthesized in NRPS (Bunet et al., 2014; Inglis et al., 2013), encompassing various functional catalytic domains responsible for the activation of the amino acid, propagation of the growing peptide chain, condensation of the amino acids and the release of peptides by hydrolysis or macrocyclization, etc. (Lee et al., 2010; Yin et al., 2013). The products of non-ribosomal synthesis generally contain atypical building blocks and their molecular weights span from 400 to 1600 Da (Meyer et al., 2008).

There are many analytical techniques for characterizing siderophores. These include CAS (Chrome azurol S) assays (Milagres, Machuca, & Napoleão, 1999), growth stimulation tests, $^{59}Fe$ uptake assays and isoelectrofocusing. Although they are fairly functional, these assays fail to give structural information and can easily be misinterpreted. In contrast siderophore analysis using mass spectrometry, NMR spectroscopy and/or X-ray diffraction (Bottcher & Clardy, 2014) allow for detailed structure analysis. In addition to screening for known siderophores, the HPLC/ESI-MS approach is extremely useful for the detection of biogenetic precursors of siderophores. As illustrative example, pyoverdins are biosynthesized by large NRPSs involving at least 12 different proteins, starting in the cytoplasm and ending in the periplasm (Parker et al., 2014). More than 60 pyoverdins have been described so far (Schalk & Guillon, 2013) and represent very complex branch-cyclic structures (Fig. 1).

Table 1 summarizes selected important microbial siderophores with their physico-chemical characteristics. Molecular formulas and IUPAC mass values of the desferri- and ferriforms ($Fe^{3+}$) of siderophores can be used for initial orientation in complex fermentation broths or clinical samples. Table 1 also reports the microbial source and original references, from which actual structures can be traced. At present, our in-house siderophore libraries contain secondary metabolites of genera *Aspergillus*, *Alternaria*, *Emericella*, *Pseudallescheria*, *Cladosporium*, *Fennellia*, *Eurotium*, *Trichothecium*, *Phoma*, *Metarhizium*, *Beauveria*, and *Candida*. This collection also contains 600 annotated microbial siderophore entries and can be provided upon request in xml or xls formats. Xml format is used in mMass open source tool, which gained reputation in lipid and proteomic analysis (Strohalm et al., 2010). The software supports general data formats and can be downloaded for free from www.mmass.org. For a typical computer screen snapshot see Figure 2. In this particular example siderophores were identified in an externally calibrated MALDI mass spectrum of a urinal sample. Mass tolerance was set to 2 ppm and no adduct formation (or iron presence) was selected. Hence, ferric form of Ferrioxamine E (m/z 654.2680) was not labeled in this case. Positive hits were annotated by green circles in the mass spectrum and listed in green in identified compound list.

For general microbial compounds, the most comprehensive commercial database is AntiBase (Wiley-VCH, Weinheim, Germany) the 2012 version of which contains 40,000 recorded compounds (http://www.wiley-vch.de/stmdata/antibase.php, access date June 26, 2014). In addition, there are many other useful repositories (KEGG, Metlin, human metabolomics database, Scifinder, Antimarin database, dictionary of natural products). However, not all of them are freely accessible from the web. Scripps center for metabolomics claims more than 240,000 metabolite entries (http://metlin.scripps.edu/index.php, access date June 27, 2014). The in-house siderophore library can also be obtained from R. Schuhmacher group, which recently published a comprehensive work on *Trichoderma* siderophores (Lehner et al., 2013). Free online siderophore library contains 262 structures with microbial source information (http://bertrandsamuel.free.fr/siderophore_base/siderophores.php, access date June 26, 2014). Chemistry and biology of siderophores covering 1950 up to the end of 2009 was reviewed by R. Hider and X. Kong. For structures see also the supplementary file available from the internet (Hider & Kong, 2010). In addition to the main document, product ion mass spectra and a lot of useful information can also be found in supplementary material from P. Dorrestein's work (Moree et al., 2012). Some commercial software tools for fast dereplication of natural products were reviewed recently (Klitgaard et al., 2014).

## III. ENRICHMENT OF SIDEROPHORES

Siderophore overproducing strains with substantial industrial importance can be found in patent literature (Weber et al., 2010). With the exception of fermentation broths the concentrations of siderophores in other real samples are low and masked by complex matrix. The removal of interfering compounds as well as pre-concentration of siderophores represent a standard step not only in clinical diagnostics (Willemse-Erix et al., 2010).

**TABLE 1.** Mass spectrometry data of selected naturally occurring siderophores

| Siderophore | Molecular formula | Theoretical masses (m/z) | | Strain or source | Ref. |
|---|---|---|---|---|---|
| | | $[M+H]^+$ | $[M+Fe-2H]^+$ | | |
| Amphibactin D | $C_{38}H_{69}N_7O_{13}$ | 832.5026 | 885.4141 | Marine water | (Gledhill et al., 2004; Mawji et al., 2008; Mawji et al., 2011) |
| Amphibactin E | $C_{40}H_{71}N_7O_{13}$ | 858.5183 | 911.4297 | Marine water | |
| Anguibactin | $C_{15}H_{16}N_4O_4S$ | 349.0965 | 402.0080 | *Vibrio anguillarum* | (Naka, Actis, & Crosa, 2013) |
| Bacillibactin | $C_{39}H_{42}N_6O_{18}$ | 883.2628 | 936.1743 | *Bacillus cereus, Bacillus anthracis* | (Zawadzka et al., 2008) |
| Bisucaberin | $C_{18}H_{32}N_4O_6$ | 401.2395 | 454.1509 | *Vibrio alginolyticus B522, Shewanella algae B516* | (Boettcher & Clardy, 2014) |
| Bisucaberin B | $C_{18}H_{34}N_4O_7$ | 419.2500 | 472.1615 | *Tenacibaculum mesophilum* | (Fujita, Nakano, & Sakai, 2013) |
| Coelichen | $C_{21}H_{39}N_7O_{11}$ | 566.2780 | 619.1895 | *Streptomyces* spp. | (Dimkpa et al., 2008) |
| Coprogen | $C_{35}H_{56}N_6O_{13}$ | 769.3978 | 822.3093 | *Laccaria laccata, Laccaria bicolor, Pseudomonas aeruginosa, Aspergillus fumigatus* | (Haselwandter et al., 2013; Hayen & Volmer, 2005) |
| Corynebactin | $C_{18}H_{26}N_2O_{14}$ | 495.1457 | 548.0571 | *Corynebacterium diphtheriae* | (Zajdowicz et al., 2012) |
| Desferrioxamine $A_{1a}$ Desferrioxamine $A_{1b}$ | $C_{24}H_{46}N_6O_8$ | 547.3450 | 600.2565 | *Salinispora tropica CNB-440* | (Ejje et al., 2013) |
| Desferrioxamine $A_2$ | $C_{23}H_{44}N_6O_8$ | 533.3293 | 586.2408 | *Salinispora tropica CNB-440* | |
| Desferrioxamine B | $C_{25}H_{48}N_6O_8$ | 561.3606 | 614.2721 | *Streptomyces* spp., *Pseudomonas aeruginosa, Aspergillus fumigatus* | (Dimkpa et al., 2008; Ejje et al., 2013; Gledhill et al., 2004; Hayen & Volmer, 2005; Mawji et al., 2011; McCormack, Worsfold, & Gledhill, 2003; Petrik et al., 2014) |
| Desferrioxamine $D_1$ | $C_{27}H_{50}N_6O_9$ | 603.3712 | 656.2827 | *Salinispora tropica CNB-440* | (Ejje et al., 2013) |
| Desferioxamine $D_2$ | $C_{26}H_{46}N_6O_9$ | 587.3399 | 640.2514 | Marine water | (Ejje et al., 2013; Mawji et al., 2011) |
| Desferioxamine E | $C_{27}H_{48}N_6O_9$ | 601.3556 | 654.2670 | *Streptomyces* spp., *Aspergillus fumigatus,* marine water | (Dimkpa et al., 2008; Ejje et al., 2013; Mawji et al., 2008; Mawji et al., 2011; Petrik et al., 2014) |
| Desferrioxamine G | $C_{27}H_{50}N_6O_{10}$ | 619.3661 | 672.2776 | *Pseudomonas stutzeri,* marine water | (Essen et al., 2007; Gledhill et al., 2004; Mawji et al., 2008; Mawji et al., 2011) |
| Desferrioxamine $G_2$ | $C_{26}H_{48}N_6O_{10}$ | 605.3505 | 658.2619 | *Pseudomonas stutzeri* | (Essen et al., 2007) |
| Desferrioxamine N | $C_{26}H_{50}N_6O_8$ | 575.3763 | 628.2878 | *Salinispora tropica CNB-440* | (Ejje et al., 2013) |
| Desferrioxamine $X_1$ | $C_{25}H_{44}N_6O_9$ | 573.3243 | 626.2357 | *Pseudomonas stutzeri* | (Essen et al., 2007) |
| 2,3-Dihydroxybenzoic acid | $C_7H_6O_4$ | 155.0339 | 207.9453 | *Escherichia coli, Bacillus DET9* | (Ma & Payne, 2012; Patel et al., 2010) |
| 2,3-Dihydroxy-benzoylglycine | $C_9H_9NO_5$ | 212.0553 | 264.9668 | *Strain ST3* | (Ahire et al., 2011b) |
| 2,3-Dihydroxy-benzoylserine | $C_{10}H_{11}NO_6$ | 242.0659 | 294.9774 | *Strain ST2* | (Ahire et al., 2011a) |
| Dimerumic acid | $C_{22}H_{36}N_4O_8$ | 485.2606 | 538.1721 | *Scedosporium apiospermum, Trichoderma* spp. | (Bertrand et al., 2009; Lehner et al., 2013) |
| Enterobactin | $C_{30}H_{27}N_3O_{15}$ | 670.1515 | 723.0630 | *Escherichia coli, Strain ST2, Pseudomonas aeruginosa, Klebsiella pneumoniae* | (Ahire et al., 2011a; Bachman et al., 2011; Hayen & Volmer, 2005; Ma & Payne, 2012) |

| | | | | | |
|---|---|---|---|---|---|
| Epichloënin A | $C_{46}H_{74}N_{12}O_{18}$ | 1083.5317 | 1136.4431 | *Epichloë festucae* | (Koulman et al., 2012) |
| Epichloënin B | $C_{44}H_{71}N_{11}O_{17}$ | 1026.5102 | 1079.4217 | *Epichloë festucae* | |
| Ferricrocin | $C_{28}H_{47}N_9O_{13}$ | 718.3366 | 771.2481 | *Laccaria laccata, Laccaria bicolor, Aspergillus fumigatus, Trichoderma* spp. | (Haselwandter et al., 2013; Lehner et al., 2013; Petrik et al., 2014) |
| Ferrichrome | $C_{27}H_{45}N_9O_{12}$ | 688.3260 | 741.2375 | *Pseudomonas aeruginosa, Aspergillus fumigatus,* marine water | (Hayen & Volmer, 2005; McCormack, Worsfold, & Gledhill, 2003; Petrik et al., 2014) |
| Ferrirhodin | $C_{41}H_{67}N_9O_{17}$ | 958.4728 | 1011.3842 | *Pseudomonas aeruginosa, Fusarium sacchari* | (Hayen & Volmer, 2005; Munawar et al., 2013) |
| Fusarinine A | $C_{22}H_{38}N_4O_9$ | 503.2712 | 556.1826 | *Trichoderma* spp. | (Lehner et al., 2013) |
| Fusarinine B | $C_{33}H_{56}N_6O_{13}$ | 745.3978 | 798.3093 | *Laccaria laccata, Laccaria bicolor, Fusarium roseum* | (Haselwandter et al., 2013) |
| Fusarinine C (cyclic fusigen) | $C_{33}H_{54}N_6O_{12}$ | 727.3873 | 780.2987 | *Laccaria laccata, Laccaria bicolor, Fusarium roseum, Aureobasidium pullutans HN6.2, Aspergillus fumigatus, Trichoderma* spp. | (Haselwandter et al., 2013; Lehner et al., 2013; Petrik et al., 2014; Wang et al., 2009) |
| Mirubactin | $C_{26}H_{32}N_6O_{11}$ | 605.2202 | 658.1316 | *Actinosynnema mirum* | (Giessen et al., 2012) |
| Mugineic acid 2'-epi-mugineic acid | $C_{12}H_{20}N_2O_8$ | 321.1292 | 374.0407 | rhizosphere | (Dell'mour et al., 2010; Dell'mour et al., 2012) |
| 2'-deoxymugineic acid | $C_{12}H_{20}N_2O_7$ | 305.1343 | 358.0458 | rhizosphere | (Dell'mour et al., 2010; Dell'mour et al., 2012; Weber, von Wiren, & Hayen, 2006) |
| $N^{\alpha}$-methyl coprogen B | $C_{34}H_{56}N_6O_{12}$ | 741.4029 | 794.3144 | *Scedosporium apiospermum* | (Bertrand et al., 2009) |
| Petrobactin | $C_{34}H_{50}N_6O_{11}$ | 719.3610 | 772.2725 | *Bacillus cereus, Bacillus anthracis, Bacillus subtilis* | (Bugdahn et al., 2010; Zawadzka et al., 2008) |
| Pseudobactin | $C_{42}H_{60}N_{12}O_{16}$ | 989.4323 | 1042.3438 | *Pseudomonas fluorescens WCS374r* | (Djavaheri et al., 2012) |
| Pseudomonine | $C_{16}H_{18}N_4O_4$ | 331.1400 | 384.0515 | *Pseudomonas fluorescens WCS374r* | |
| Putrebactin | $C_{16}H_{28}N_4O_6$ | 373.2082 | 426.1196 | *Shewanella putrefaciens* | (Soe & Codd, 2014) |
| Quinolobactin | $C_{11}H_9NO_4$ | 220.0604 | 272.9719 | *Pseudomonas fluorescens ATCC 17400* | (Mossialos et al., 2000) |
| Rhizoferrin | $C_{16}H_{24}N_2O_{12}$ | 437.1402 | 490.0517 | *Francisella tularensis* | (Sullivan et al., 2006) |
| Rhodobactin | $C_{36}H_{50}N_{10}O_{13}$ | 831.3632 | 884.2746 | *Rhodococcus rhodochrous* | (Dhungana et al., 2007) |
| Rhodotorulic acid | $C_{14}H_{24}N_4O_6$ | 345.1769 | 398.0883 | *Pseudomonas aeruginosa,* marine water | (Hayen & Volmer, 2005; McCormack, Worsfold, & Gledhill, 2003) |
| Salicylic acid | $C_7H_6O_3$ | 139.0390 | 191.9504 | *Pseudomonas fluorescens WCS374r* | (Djavaheri et al., 2012) |
| Salmochelin S1 | $C_{26}H_{30}N_2O_{16}$ | 627.1668 | 680.0783 | *Escherichia coli* | (Caza et al., 2008) |
| Salmochelin S2 | $C_{42}H_{49}N_3O_{26}$ | 1012.2677 | 1065.1792 | *Escherichia coli* | |
| Salmochelin S4 | $C_{42}H_{47}N_3O_{25}$ | 994.2571 | 1047.1686 | *Escherichia coli* | |
| Salmochelin SX | $C_{16}H_{21}NO_{11}$ | 404.1187 | 457.0302 | *Escherichia coli* | |

| | | | | | |
|---|---|---|---|---|---|
| Scabichelin | $C_{26}H_{49}N_9O_{10}$ | 648.3680 | 701.2795 | *Streptomyces antibioticus NBRC 13838, Streptomyces scabies JCM 7914, Streptomyces turgidiscabies JCM 10429* | (Kodani et al., 2013) |
| Staphyloferrin A | $C_{17}H_{24}N_2O_{14}$ | 481.1300 | 534.0415 | *Staphylococcus aureus* | (Pandey, Jarvis, & Low, 2014) |
| Staphyloferrin B | $C_{16}H_{24}N_4O_{11}$ | 449.1514 | 502.0629 | *Ralstonia solanacearum* | (Bhatt & Denny, 2004) |
| Synechobactin A | $C_{22}H_{40}N_4O_9$ | 505.2868 | 558.1983 | *Synechococcus sp. PCC 7002* | (Boiteau et al., 2013) |
| Synechobactin B | $C_{24}H_{44}N_4O_9$ | 533.3181 | 586.2296 | *Synechococcus sp. PCC 7002* | |
| Synechobactin C | $C_{26}H_{48}N_4O_9$ | 561.3494 | 614.2609 | *Synechococcus sp. PCC 7002* | |
| N,N',N''-triacetylfusarinine C | $C_{39}H_{60}N_6O_{15}$ | 853.4189 | 906.3304 | *Laccaria laccata, Laccaria bicolor, Aspergillus fumigatus* | (Haselwandter et al., 2013; Petrik et al., 2014) |
| Turgichelin | $C_{24}H_{44}N_8O_{11}$ | 621.3207 | 674.2322 | *Streptomyces antibioticus NBRC 13838, Streptomyces scabies JCM 7914, Streptomyces turgidiscabies JCM 10429* | (Kodani et al., 2013) |
| Vanchrobactin | $C_{16}H_{23}N_5O_7$ | 398.1670 | 451.0785 | *Vibrio anguillarum* | (Naka, Lopez, & Crosa, 2008) |
| Vicibactin | $C_{33}H_{54}N_6O_{15}$ | 775.3720 | 828.2835 | *Rhizobium leguminosarum ATCC14479* | (Wright et al., 2013) |
| Yersiniabactin | $C_{21}H_{27}N_3O_4S_3$ | 482.1236 | 535.0351 | *Klebsiella pneumoniae* | (Bachman et al., 2011) |

Table 2 summarizes literature data indicating the application of solid phase extraction of specific molecular structures. The most popular sorbents were polystyrene-divinylbenzene copolymers represented by Amberlite XAD-2, Amberlite XAD-4, Amberlite XAD 16 commercial cartridges. For some structures modified polystyrene-divinylbenzene copolymers were found superior. For eluents suitable for hydroxylated (Isolute ENV+ cartridge), co-polymeric divinylbenzene and N-vinylpyrrolidone (Oasis HLB 12 cc cartridges), acrylic ester resins (Amberlite XAD-7 cartridge) or silica based bonded phases (Sep-Pak $C_{18}$ plus cartridge) see Table 2 and references cited therein. For explorative SPE for accelerated microbial natural product discovery see references (Mansson et al., 2010; Nielsen et al., 2011).

Significantly, currently there is paucity of enrichment strategies targeting specific valence of iron utilizing more specific iron bonding. An affinity ferrous-form siderophore capture could potentially be carried out by Smopex-102 fibers acting as metal scavengers (Karppi et al., 2009). Chopped fibers weak acid cation exchangers based on acrylic acid grafted polyolefins (exchange capacity 7–10 mmol/g) can also be potentially tested (http://www.scavengingtechnologies.com/, access date June 25, 2014).

## IV. CHARACTERIZATION OF SIDEROPHORES BY MOLECULAR MASS SPECTROMETRY

The applications of mass defect data filtering was reviewed by Sleno (2012). In ESI or MALDI mass spectra both desferric and ferric forms of siderophores can be observed (Fig. 3, insets). The iron signature can be inferred even from low resolution mass spectrum due to stable isotope profile [naturally occurring isotopes: $^{54}$Fe (5.8%), $^{56}$Fe (91.8%), $^{57}$Fe (2.1%), and $^{58}$Fe (0.3%)]. In iron specific case interpreter tools search for 1.99533 or 52.91146 m/z differences between isotopic ($^{54}$Fe, $^{56}$Fe) signals or desferric and ferric form of a siderophore, respectively (Yin et al., 2013). Siderophore structural details are then obtained from the product ion scanning. Figure 1 indicates dissociation of amidic bonds in ferric form of ferrioxamine B. For m/z values of protonated molecules and $[M+Fe-2H]^+$ ions of selected siderophores see Table 1.

Figure 4 illustrates the hydrogen index as a function of the oxygen/carbon (oxygen index) and nitrogen/carbon atomic ratios of carbon-containing both desferric and ferric forms of siderophores. Van Krevelen plots were generated *in silico* from the siderophore set listed in Table 1. Desferric forms have higher indexes than their ferric forms from definition. Note the non-constant differences between the ferric and desferric form

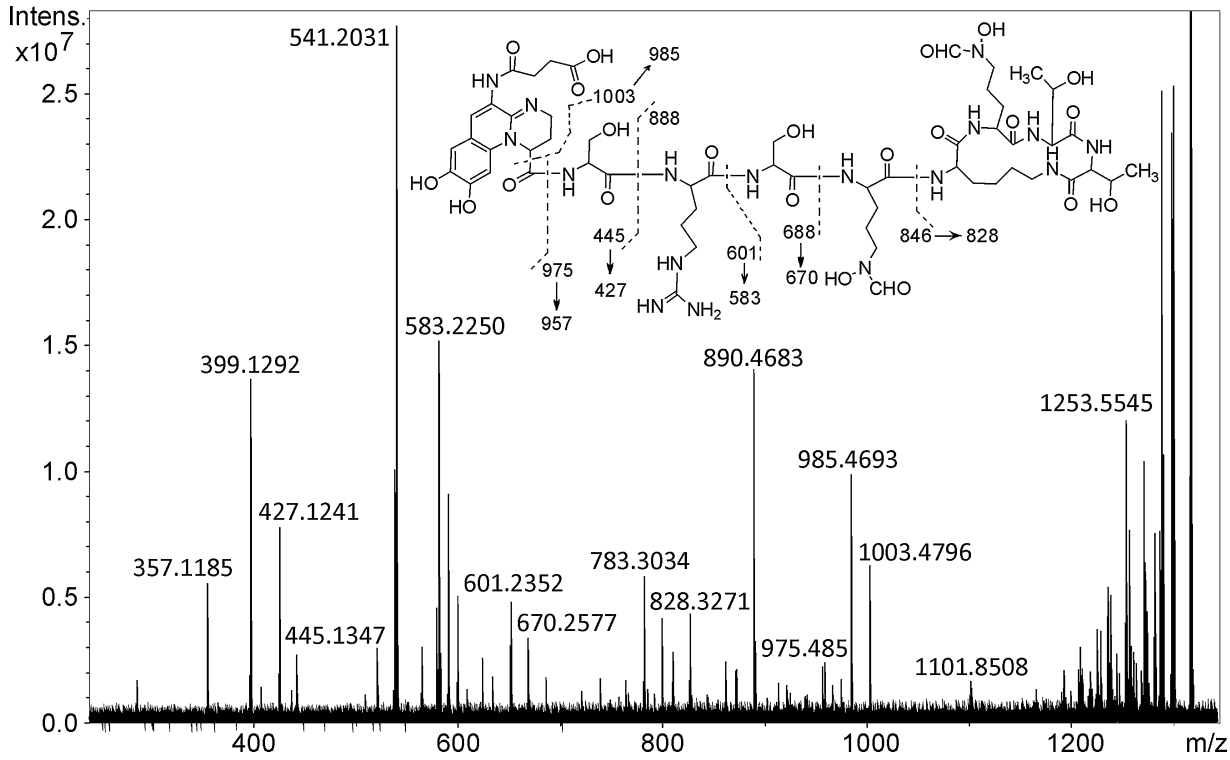


**FIGURE 1.** Fragmentation of Pyoverdin Pa A.

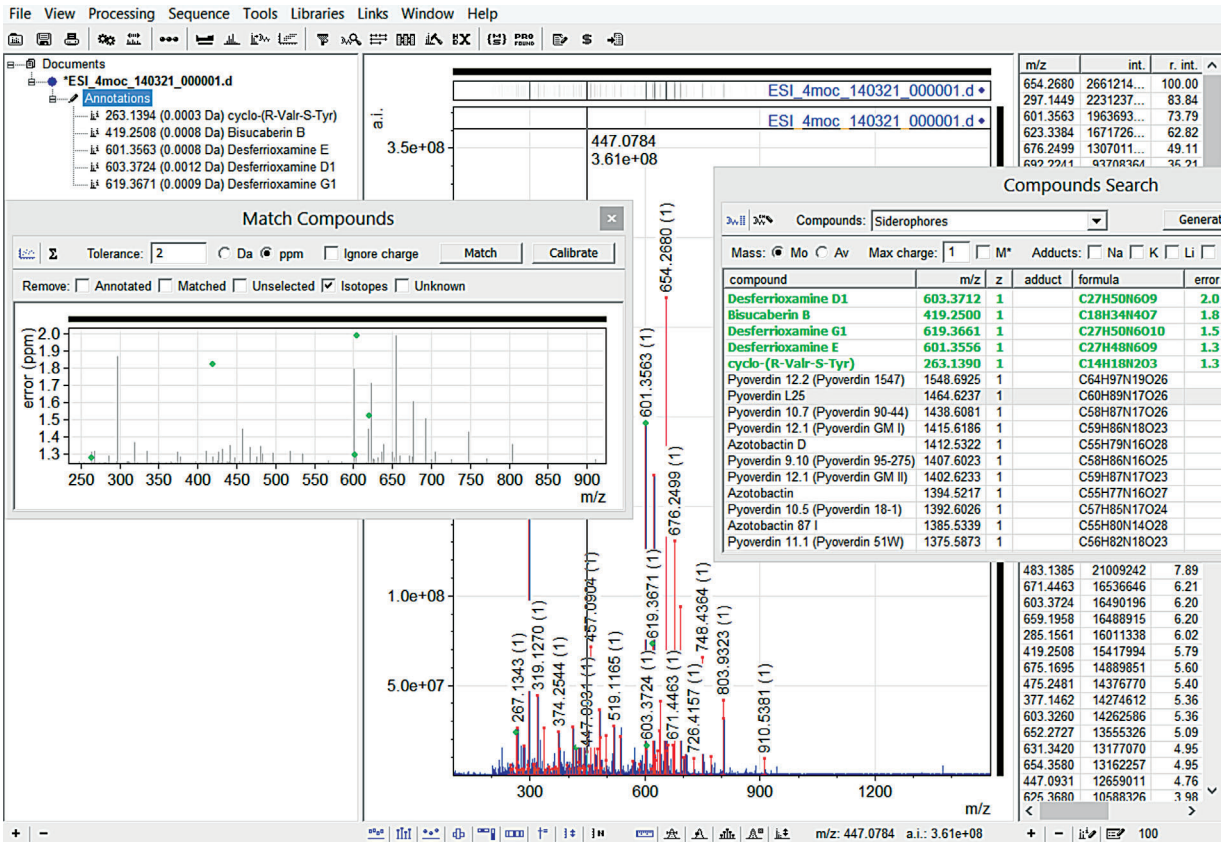


**FIGURE 2.** Snapshot of mMass application.

**TABLE 2.** Protocols for solid phase extraction of microbial siderophores

| SPE cartridge | Analyte | Eluent | Ref. |
|---|---|---|---|
| Isolute ENV+ | epichloënin A | methanol | (Lee et al., 2010) |
| | epichloënins A, B | formic acid : water : methanol 1:20:80 (v/v/v) | (Koulman et al., 2012,Lee et al., 2010) |
| | synechobactins A, B, C ferrioxamine E, ferrichrome | methanol | (Boiteau et al., 2013) |
| | amphibactins D and E, ferrioxamine B, ferrioxamines $D_2$, E, G | acetonitrile : propan-2-ol : water : formic acid 81:14:5:1 (v/v/v/v) | (Mawji et al., 2008,Mawji et al., 2011) |
| | amphibactins D, and E ferrioxamine B, and G | formic acid : water : methanol 1:20:80 (v/v/v) | (Gledhill et al., 2004) |
| | ferrichrome, ferrioxamine B, rhodotorulic acid | formic acid : water : methanol 1:20:80 (v/v/v) | (McCormack, Worsfold, & Gledhill, 2003) |
| Amberlite XAD-2 | coprogen, ferricrocin, fusarinine B, fusarinine C, N,N',N''-triacetylfusarinine C | methanol | (Haselwandter et al., 2013) |
| | ferrioxamines $A_{1a}$, $A_{1b}$, $A_2$, B, $D_1$, $D_2$, E, N | 50 % methanol and 100 % methanol | (Ejje et al., 2013) |
| Amberlite XAD-7 | anguibactin, vanchrobactin | methanol | (Naka, Lopez, & Crosa, 2008) |
| | rhodobactin | 1 % TFA in10 % methanol | (Dhungana et al., 2007) |
| Amberlite XAD-16 | "Hydroxamate-type" siderophores | methanol | (McMillan et al., 2010,Velasquez et al., 2011) |
| Amberlite XAD-4 | pyoverdins | 50 % methanol | (Murugappan et al., 2012) |
| Sep-Pak $C_{18}$ plus | ferrioxamines B, E, G, $G_2$, $X_1$ | methanol | (Lee et al., 2010) |
| Oasis HLB 12 cc | coprogen, enterobactin, ferrioxamine B, ferrichrome, ferrirhodin, pyochelin, rhodotorulic acid | 2 % formic acid in methanol | (Hayen & Volmer, 2005) |

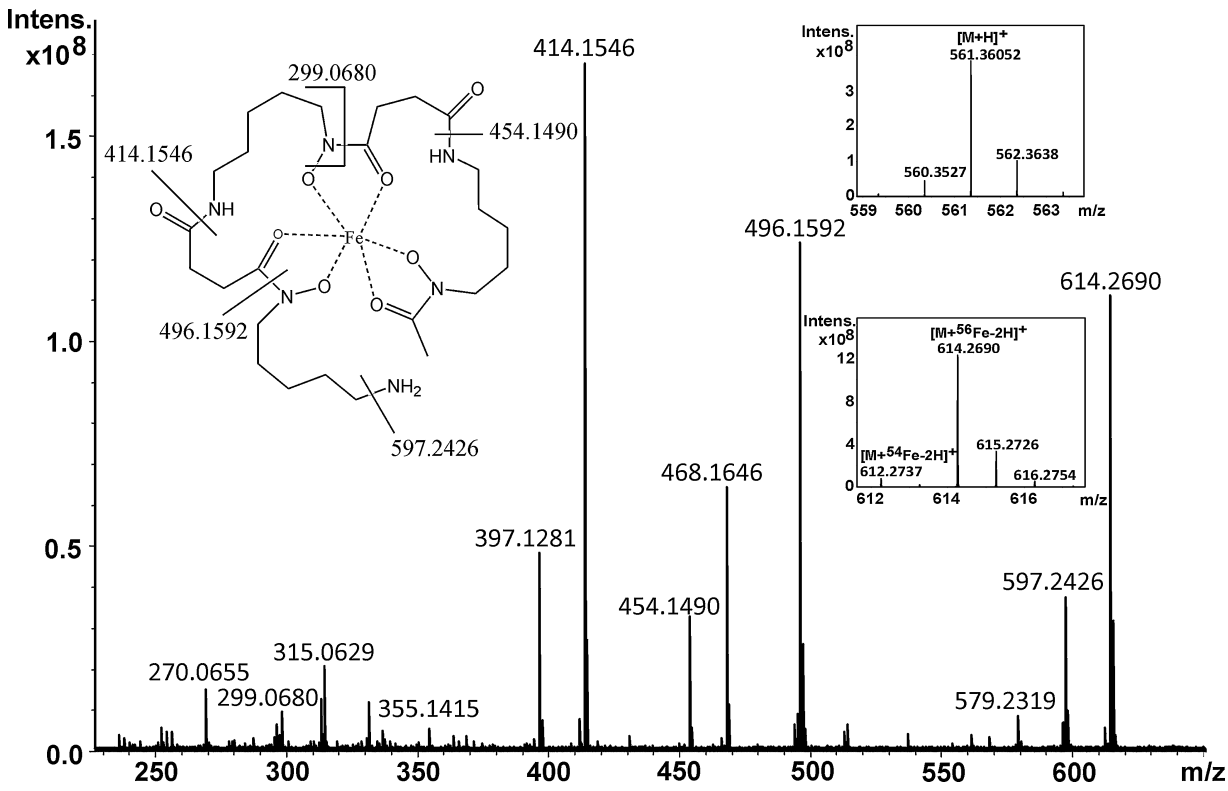


**FIGURE 3.** The product ion spectrum of ferrioxamine B $[M+^{56}Fe\text{-}2H]^+$ ion (m/z 614.2721, isolation window 5 Da). The insets show details of molecular regions of desferric (top) and ferric forms (bottom) recorded in the conventional mass spectrum.

of a selected siderophore. Clustering the siderophores into families according to oxygen index is depicted in Figure 5. The broad distribution of bactins (1) well corresponds to their structural diversity. On the contrary, ferrioxamines (2) are more homogeneous in their elemental composition (Table 1). Van Krevelen plots can be used for initial orientation in and dataset presentation of complex fermentation broths.

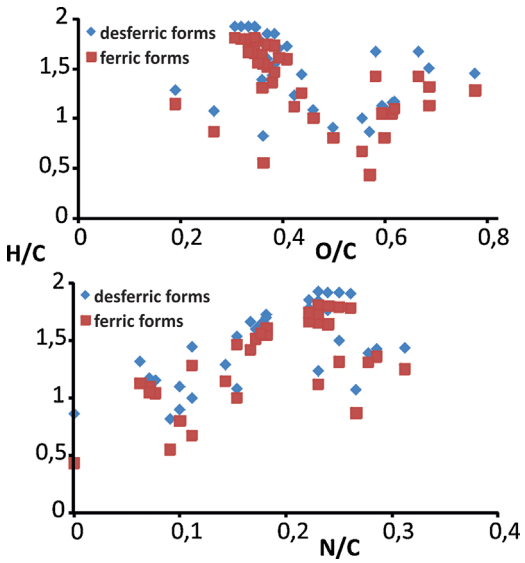


**FIGURE 4.** Dirk Willem van Krevelen's H/C over O/C (top) and N/C (bottom) diagrams illustrating the distribution of desferric and ferric forms in siderophore space. Individual siderophores were extracted from Table 1.

In addition to stable isotopes, $^{59}$Fe-labeling was also used in biochemical studies (Expert, Boughammoura, & Franza, 2008). The monitoring the $^{59}$Fe-labeled fermentation broths can be directly carried out by liquid chromatography with radiodetection (Budzikiewicz, Schafer, & Meyer, 2007). The total number of references related to $^{59}$Fe-labeling is rather low and may be attributed to the introduction of inductively coupled plasma mass spectrometry (ICP-MS) applications.

## V. THE CONTRIBUTION OF ICP-MS AND ATOMIC SPECTROMETRY TECHNIQUES TO SIDEROPHORE CHARACTERIZATION

Inductively coupled plasma mass spectrometry offers many unique advantages over other techniques for analysis of metal-complexed biomolecules like siderophores. The first advantage is high temperature ionization (approximately 5,500 K) over low-temperature ion sources, resulting in decomposition of all chemical bonds in the analyte plasma. Therefore, the data acquired from a plasma ion source represent the total content of an element in the sample, enabling simple and accurate multielement quantitation. Conventional ICP-MS generates mass spectra in the mass-to-charge ($m/z$) range 5–257. A second advantage of ICP-MS is the analyte plasma has the high ion density, provides excellent collision rates and therefore also higher sensitivities than some other ion sources. The ICP ion source is also less vulnerable to the salts and solvents usually

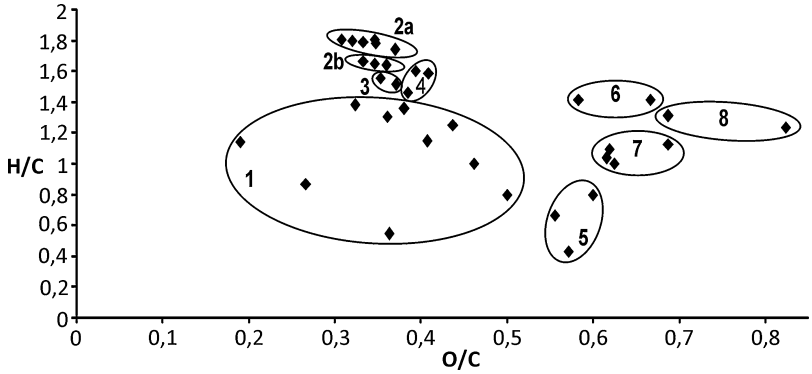


**FIGURE 5.** Two-dimensional van Krevelen's diagram indicating the clustering of siderophore families extracted from Table 1: 1-bactins, 2a-linear ferrioxamines, 2b-cyclic ferrioxamines, 3-coprogens, 4-fusarinines, 5-2,3-dihydroxy derivatives (benzoic acid, glycine, and serine), 6-mugineic acids, 7-salmochelins, 8-staphyloferrins.

present in biological samples. In combination with HPLC the ICP-MS thus represents a good tool for locating ferric forms of siderophores in complex sample mixtures.

According to recent report sensitive detection (<1 picomole Fe) of siderophores can be achieved by using iron-free HPLC systems to reduce background Fe levels (Boiteau et al., 2013). In that report the $^{40}Ar^{16}O^{+}$ interferences were minimized on $^{56}Fe$ by application of a collision cell and introducing oxygen into the sample carrier gas to prevent the formation of carbon deposits that decrease sensitivity. HPLC-ICP mass spectrometry in low organic solvent systems can also be used for ratio determination of bound and free iron in clinical samples. The addition of pyridine-2,6-dicarboxylic acid into the mobile phase and the resulting anionic complexes were separated by ion exchange chromatography (IonPac Cs-5A column) followed by ICP-MS detection (Hu, 2011). An older alternative based on reductive displacement of iron by gallium was performed using ascorbate as the reducing agent to increase the sensitivity. Nanomolar detection limits were achieved in this case (Moberg et al., 2004).

Six free metals [Co(II), Cu(II), Fe(III), Mn(II), Ni(II), and Zn(II)] together with their complexes with phytosiderophores (mugineic acid, epi-mugineic acid and deoxymugineic acid and their diastereomers) were analyzed by capillary electrophoresis (CE) and sector field ICP-MS (Dell'mour et al., 2010). CE separation was realized at a voltage of +25 kV employing a background electrolyte containing 20 mM ammonium bicarbonate at pH 7.2. Limits of detection of $[M\text{-}4H+Fe(III)]^{-}$ ions were in 0.9–2.2 μM range. Slightly better sensitivity was achieved in negative ion mode for the corresponding desferric forms (0.8–1.4 μM).

Phytoremediation is another important area of siderophore industrial applications. Inductively coupled plasma mass spectrometry was used to measure iron and cadmium contents in the bacterium *Streptomyces tendae* and in sunflower plant grown in Cd-amended soil (Dimkpa et al., 2009b). It was concluded that siderophores can help reduce toxic metal uptake in bacteria, while simultaneously facilitating the uptake of such metals by plants.

High-precision isotopic analyses by multicollector ICP-MS were used to investigate the mass-dependent fractionation of Fe isotopes during bacterial metal assimilation in experiments with *Azotobacter vinelandii*. *A. vinelandii* is a diazotroph with high demand for iron during nitrogen fixation. The growth medium became isotopically lighter as Fe was removed from solution. The experimental data were interpreted in terms of Rayleigh fractionation, yielding fractionation factor of 1.0011 for iron (Wasylenki et al., 2007).

Alternatively, iron content in siderophore samples can be determined by graphite furnace atomic absorption spectrometry (Lehner et al., 2013). Eighteen different iron chelators isolated from *Trichoderma* spp. were detected and ten structures characterized by mass spectrometry.

## VI. MASS SPECTROMETRY IN MEDICINAL APPLICATIONS OF SIDEROPHORES

Resistance to antibiotics was revealed by the monitoring of characteristic mass shifts of microorganism biomarkers in mass spectra of vegetative cells and spores grown with/without antibiotics in a $^{13}C$-labeled/non-labeled media (Demirev et al., 2013). The presence of small acid-soluble spore proteins generated in the presence of an antibiotic in 2 hr frame was a resistance indicator. In tackling antibiotic resistance the three siderophore-related approaches were developed: competitive iron chelation, blocking of siderophore biosynthesis, and finally the development of siderophore-drug conjugates called *Trojan horse antibiotics* as new promising drugs capable to combat infections caused by resistant bacteria and fungi (Costa Mattos et al., 2013; Ji & Miller, 2012; Wencewicz et al., 2009). The considerable antibacterial activity against ESKAPE pathogens (*Enterococcus faecium*, *Staphylococccus aureus*, *Klebsiella pneumonia*, *Acinetobacter baumannii*, *Pseudomonas aeruginosa*, *Enterobacter aerogenes*, and *Escherichia coli*) was revealed by desferrioxamine, sideromycins or staphyloferrin A conjugates (Milner et al., 2013; Wencewicz & Miller, 2013; Flanagan et al., 2011; Tomaras et al., 2013). Baulamycins A and B were identified as inhibitors of siderophore biosynthesis in *Staphylococcus aureus* and *Bacillus anthracis*. Their excellent antibacterial activity against Gram-positive and Gram-negative bacteria represented the potential of siderophores as broad-spectrum antibiotics (Tripathi et al., 2014).

Mass spectrometry imaging (MSI) experiments provide direct access inhibition constants in antimicrobial susceptibility studies (Moree et al., 2013). The interaction between combating microorganisms through siderophore equipment was also

assessed by MSI (Moree et al., 2012; Yang et al., 2011). Mass spectrometry imaging was applied for the determination of secondary metabolites of worldwide collected yeast, filamentous fungi, pathogens, and marine-derived bacteria including *Streptomyces coelicolor*, *Bacillus subtilis*, *Pseudomonas aeruginosa* (Hsu et al., 2013). The determination and visualization of metabolites of *Pseudomonas aeruginosa* and *Aspergillus fumigatus* causing polymicrobial infection in patients with cystic fibrosis was another exciting application of MSI (Moree et al., 2012).

In fully sequenced microorganisms many siderophore receptors have been characterized by mass spectrometry (Mathavan et al., 2014; Podkowa et al., 2014). The receptor proteins are synthesized in response to iron limitation and may become major outer membrane proteins with copy numbers up to $10^5$. Siderophore-transport processes may or may not involve the permeation of the complex in ferric form through the cell membrane into cytoplasm. The desferric siderophore is rapidly excreted making it an attractive diagnostic biomarker molecule (Petrik et al., 2014).

To conclude, siderophores represent very exciting family of metal chelators that have extremely broad spectrum of biological activities and functions with an array of important medical, biochemical, geochemical, and agricultural applications. Although not possessing simple organic structures, mass spectrometry has contributed significantly to the fields of siderophore inorganic and molecular analytical chemistries in past five years. This paper represents the first mass spectrometry review in the field of microbial siderophores highlighting their emerging applications and medical importance.

## VII. ABBREVIATIONS

| | |
|---|---|
| CAS | chrome azurol S |
| CE | capillary electrophoresis |
| ESI-MS | electrospray ionization mass spectrometry |
| FOXE | ferrioxamine E |
| HPLC | high performance liquid chromatography |
| ICP-MS | inductively coupled plasma mass spectrometry |
| MC-ICP-MS | multicollector inductively coupled plasma mass spectrometry |
| MRI | magnetic resonance imaging |
| MSI | mass spectrometry imaging |
| NMR | nuclear magnetic resonance |
| SPE | solid phase extraction |
| TAFC | triacetylfusarinine C |

## ACKNOWLEDGMENTS

The work was supported by Operational programs Research, development and innovations and Prague – Competitiveness (projects CZ.1.05/2.1.00/03.0058 and CZ.2.16/3.1.00/24023, respectively). The authors thank Dr. Andrea Palyzova (IMIC Prague) and Milos Petrik (Biomedreg Olomouc) for providing siderophore standards. The authors also acknowledge the support from the Ministry of Education, Youth and Sports of the Czech Republic (LD13038), Czech Science Foundation (P206/12/1150), IMIC institutional research concept RVO61388971 and Palacký University (project IGA_PrF_2014031).

## REFERENCES

Asmathunisha N, Kathiresan K. 2013. A review on biosynthesis of nanoparticles by marine organisms. Colloids Surf B Biointerfaces 103:283–287.

Bassetti M, Merelli M, Temperoni C, Astilean A. 2013. New antibiotics for bad bugs: Where are we? Ann Clin Microbiol Antimicrob 12:15.

Bertrand S, Larcher G, Landreau A, Richomme P, Duval O, Bouchara JP. 2009. Hydroxamate siderophores of *Scedosporium apiospermum*. Biometals 22:1019–1029.

Bhainsa KC, D'Souza SF. 2006. Extracellular biosynthesis of silver nanoparticles using the fungus Aspergillus fumigatus. Colloids Surf B Biointerfaces 47:160–164.

Birus M, Gabricevic M, Kronja O, Klaic B. 1995. C-13 and H-1 NMR line broadening in desferrioxamine-b spectra - kinetics and mechanism of siderophore chemistry. Inorg Chem 34:3110–3113.

Boiteau RM, Fitzsimmons JN, Repeta DJ, Boyle EA. 2013. Detection of iron ligands in seawater and marine cyanobacteria cultures by high-performance liquid chromatography-inductively coupled plasma-mass spectrometry. Anal Chem 85:4357–4362.

Bottcher T, Clardy J. 2014. A Chimeric siderophore halts swarming vibrio. Angew Chem Int Edit 53:3510–3513.

Brard L, Granai CO, Swamy N. 2006. Iron chelators deferoxamine and diethylenetriamine pentaacetic acid induce apoptosis in ovarian carcinoma. Gynecol Oncol 100:116–127.

Budzikiewicz H, Schafer M, Meyer JM. 2007. Siderotyping of fluorescent pseudomonads - Problems in the determination of molecular masses by mass spectrometry. Mini Rev Org Chem 4:246–253.

Bunet R, Riclea R, Laureti L, Hotel L, Paris C, Girardet J-M, Spiteller D, Dickschat JS, Leblond P, Aigle B. 2014. A single Sfp-Type phosphopantetheinyl transferase plays a major role in the biosynthesis of PKS and NRPS derived metabolites in streptomyces ambofaciens AT CC23877. Plos One 9.

Costa Mattos AL, Leopoldo Constantino VR, Alves de Couto RA, Luna Pinto DM, Kaneko TM, Esposito BP. 2013. Desferrioxamine-cadmium as a 'Trojan horse' for the delivery of Cd to bacteria and fungi. J Trace Elem Med Biol 27:103–108.

Dell'mour M, Koellensperger G, Quirino JP, Haddad PR, Stanetty C, Oburger E, Puschenreiter M, Hann S. 2010. Complexation of metals by phytosiderophores revealed by CE-ESI-MS and CE-ICP-MS. Electrophoresis 31:1201–1207.

Demirev PA, Hagan NS, Antoine MD, Lin JS, Feldman AB. 2013. Establishing drug resistance in microorganisms by mass spectrometry. J Am Soc Mass Spectrom 24:1194–1201.

Dimkpa CO, Merten D, Svatos A, Buchel G, Kothe E. 2009a. Metal-induced oxidative stress impacting plant growth in contaminated soil is alleviated by microbial siderophores. Soil Biol Biochem 41:154–162.

Dimkpa CO, Merten D, Svatos A, Buchel G, Kothe E. 2009b. Siderophores mediate reduced and increased uptake of cadmium by Streptomyces tendae F4 and sunflower (Helianthus annuus), respectively. J Appl Microbiol 107:1687–1696.

Ding P, Helquist P, Miller MJ. 2008. Design and synthesis of a siderophore conjugate as a potent PSMA inhibitor and potential diagnostic agent for prostate cancer. Biorg Med Chem 16:1648–1657.

Duckworth OW, Holmstrom SJM, Pena J, Sposito G. 2009. Biogeochemistry of iron oxidation in a circumneutral freshwater habitat. Chem Geol 260:149–158.

Expert D, Boughammoura A, Franza T. 2008. Siderophore-controlled iron assimilation in the enterobacterium erwinia chrysanthemi evidence for the involvement of bacterioferritin and the suf iron-sulfur cluster assembly machinery. J Biol Chem 283:36564–36572.

Fernandes P, de Carvalho CCCR. 2014. Siderophores as "Trojan Horses": Tackling multidrug resistance? Antimicrob Resist Chemother 5:290.

Flanagan ME, Brickner SJ, Lall M, Casavant J, Deschenes L, Finegan SM, George DM, Granskog K, Hardink JR, Huband MD, Thuy H, Lamb L, Marra A, Mitton-Fry M, Mueller JP, Mullins LM, Noe MC, O'Donnell

JP, Pattavina D, Penzien JB, Schuff BP, Sun J, Whipple DA, Young J, Gootz TD. 2011. Preparation, gram-negative antibacterial activity, and hydrolytic stability of novel siderophore-conjugated monocarbam diols. Acs Med Chem Lett 2:385–390.

Franke J, Ishida K, Hertweck C. 2014. Evolution of siderophore pathways in human pathogenic bacteria. J Am Chem Soc 136:5599–5602.

Haas H. 2012. Iron - a key nexus in the virulence of *Aspergillus fumigatus*. Frontiers Microbiol 3:1–9.

Haas H, Eisendle M, Turgeon BG. 2008. Siderophores in fungal physiology and virulence. Annu Rev Phytopathol 46:149–187.

Hider RC, Kong XL. 2010. Chemistry and biology of siderophores. Nat Prod Rep 27:637–657.

Hsu C-C, ElNaggar MS, Peng Y, Fang J, Sanchez LM, Mascuch SJ, Moller KA, Alazzeh EK, Pikula J, Quinn RA, Zeng Y, Wolfe BE, Dutton RJ, Gerwick L, Zhang L, Liu X, Mansson M, Dorrestein PC. 2013. Real-time metabolomics on living microorganisms using ambient electrospray ionization flow-probe. Anal Chem 85:7014–7018.

Hu Q. 2011. Simultaneous separation and quantification of iron and transition species using LC-ICP-MS. Am J Anal Chem 2:675–682.

Inglis DO, Binkley J, Skrzypek MS, Arnaud MB, Cerqueira GC, Shah P, Wymore F, Wortman JR, Sherlock G. 2013. Comprehensive annotation of secondary metabolite biosynthetic genes and gene clusters of *Aspergillus nidulans*, *A. fumigatus*, *A. niger* and *A. oryzae*. Bmc Microbiol 13:23.

Ji C, Miller MJ. 2012. Chemical syntheses and *in vitro* antibacterial activity of two desferrioxamine B-ciprofloxacin conjugates with potential esterase and phosphatase triggered drug release linkers. Bioorg Med Chem 20:3828–3836.

Kalb D, Lackner G, Hoffmeister D. 2013. Fungal peptide synthetases: an update on functions and specificity signatures. Fungal Biol Rev 27:43–50.

Karppi J, Akerman S, Akerman K, Kontturi K, Nyyssonen K, Penttila I. 2009. Suitability of smopex (R)-102 cation-exchange fiber for analytical purposes and drug monitoring. Pharmazie 64:14–18.

Keeler BD, Brookes MJ. 2013. Iron chelation: A potential therapeutic strategy in oesophageal cancer. British Journal of Pharmacology 168:1313–1315.

Kellerschierlein W, Hagmann L, Zahner H, Huhn W. 1988. Metabolic products from microorganisms 250. Maduraferrin, a novel siderophore from actinomadura-madurae. Helv Chim Acta 71:1528–1540.

Klitgaard A, Iversen A, Andersen MR, Larsen TO, Frisvad JC, Nielsen KF. 2014. Aggressive dereplication using UHPLC-DAD-QTOF: Screening extracts for up to 3000 fungal secondary metabolites. Anal Bioanal Chem 406:1933–1943.

Kolinko I, Lohsse A, Borg S, Raschdorf O, Jogler C, Tu Q, Posfai M, Tompa E, Plitzko JM, Brachmann A, Wanner G, Mueller R, Zhang Y, Schueller D. 2014. Biosynthesis of magnetic nanostructures in a foreign organism by transfer of bacterial magnetosome gene clusters. Nature Nanotechnol 9:193–197.

Lee TV, Johnson LJ, Johnson RD, Koulman A, Lane GA, Lott JS, Arcus VL. 2010. Structure of a eukaryotic nonribosomal peptide synthetase adenylation domain that activates a large hydroxamate amino acid in siderophore biosynthesis. J Biol Chem 285:2415–2427.

Lehner SM, Atanasova L, Neumann NKN, Krska R, Lemmens M, Druzhinina IS, Schuhmacher R. 2013. Isotope-assisted screening for iron-containing metabolites reveals a high degree of diversity among known and unknown siderophores produced by *Trichoderma spp*. Appl Environ Microbiol 79:18–31.

Mansson M, Phipps RK, Gram L, Munro MHG, Larsen TO, Nielsen KF. 2010. Explorative solid-phase extraction (E-SPE) for accelerated microbial natural product discovery, dereplication, and purification. J Nat Prod 73:1126–1132.

Mathavan I, Zirah S, Mehmood S, Choudhury HG, Goulard C, Li Y, Robinson CV, Rebuffat S, Beis K. 2014. Structural basis for hijacking siderophore receptors by antimicrobial lasso peptides. Nat Chem Biol 10:340–U123.

Meyer J-M, Gruffaz C, Raharinosy V, Bezverbnaya I, Schaefer M, Budzikiewicz H. 2008. Siderotyping of fluorescent *Pseudomonas*: molecular mass determination by mass spectrometry as a powerful pyoverdine siderotyping method. Biometals 21:259–271.

Milagres AM, Machuca A, Napoleão D. 1999. Detection of siderophore production from several fungi and bacteria by a modification of chrome azurol S (CAS) agar plate assay. J Microbiol Methods 37:1–6.

Miller MJ, Zhu H, Xu Y, Wu C, Walz AJ, Vergne A, Roosenberg JM, Moraski G, Minnick AA, McKee-Dolence J, Hu J, Fennell K, Kurt Dolence E, Dong L, Franzblau S, Malouin F, Mollmann U. 2009. Utilization of microbial iron assimilation processes for the development of new antibiotics and inspiration for the design of new anticancer agents. Biometals 22:61–75.

Milner SJ, Seve A, Snelling AM, Thomas GH, Kerr KG, Routledge A, Duhme-Klair A-K. 2013. Staphyloferrin A as siderophore-component in fluoroquinolone-based Trojan horse antibiotics. Org Biomol Chem 11:3461–3468.

Moberg M, Nilsson EM, Holmstrom SJM, Lundstrom US, Pettersson J, Markides KE. 2004. Fingerprinting metal-containing biomolecules after reductive displacement of iron by gallium and subsequent column-switched LC-ICPMS analysis applied on siderophores. Anal Chem 76:2618–2622.

Moree WJ, Phelan VV, Wu CH, Bandeira N, Cornett DS, Duggan BM, Dorrestein PC. 2012. Interkingdom metabolic transformations captured by microbial imaging mass spectrometry. Proc Natl Acad Sci USA 109:13811–13816.

Moree WJ, Yang JY, Zhao X, Liu W-T, Aparicio M, Atencio L, Ballesteros J, Sanchez J, Gavilan RG, Gutierrez M, Dorrestein PC. 2013. Imaging mass spectrometry of a coral microbe interaction with fungi. J Chem Ecol 39:1045–1054.

Morgenthau A, Beddek A, Schryvers AB. 2014. The negatively charged regions of lactoferrin binding protein B, an adaptation against antimicrobial peptides. Plos One 9.

Nielsen KF, Mansson M, Rank C, Frisvad JC, Larsen TO. 2011. Dereplication of microbial natural products by LC-DAD-TOFMS. J Nat Prod 74:2338–2348.

Parker DL, Lee S-W, Geszvain K, Davis RE, Gruffaz C, Meyer J-M, Torpey JW, Tebo BM. 2014. Pyoverdine synthesis by the Mn(II)-oxidizing bacterium *Pseudomonas putida* GB-1. Frontiers Microbiol 5:1–10.

Petrik M, Haas H, Dobrozemsky G, Lass-Florl C, Helbok A, Blatzer M, Dietrich H, Decristoforo C. 2010. Ga-68-siderophores for PET imaging of invasive pulmonary aspergillosis: Proof of principle. J Nucl Med 51:639–645.

Petrik M, Haas H, Laverman P, Schrettl M, Franssen GM, Blatzer M, Decristoforo C. 2014. Ga-68-triacetylfusarinine C and Ga-68-ferrioxamine E for aspergillus infection imaging: Uptake specificity in various microorganisms. Mol Imaging Biol 16:102–108.

Podkowa KJ, Briere LAK, Heinrichs DE, Shilton BH. 2014. Crystal and solution structure analysis of FhuD2 from *Staphylococcus aureus* in multiple unliganded conformations and bound to ferrioxamine-B. Biochemistry 53:2017–2031.

Schalk IJ, Guillon L. 2013. Pyoverdine biosynthesis and secretion in *Pseudomonas aeruginosa*: implications for metal homeostasis. Environ Microbiol 15:1661–1673.

Siponen MI, Legrand P, Widdrat M, Jones SR, Zhang W-J, Chang MCY, Faivre D, Arnoux P, Pignol D. 2013. Structural insight into magnetochrome-mediated magnetite biomineralization. Nature 502:681–584.

Sleno L. 2012. The use of mass defect in modern mass spectrometry. J Mass Spectrom 47:226–236.

Strohalm M, Kavan D, Novak P, Volny M, Havlicek V. 2010. mMass 3: A cross-platform software environment for precise analysis of mass spectrometric data. Anal Chem 82:4648–4651.

Tomaras AP, Crandon JL, McPherson CJ, Banevicius MA, Finegan SM, Irvine RL, Brown MF, O'Donnell JP, Nicolau DP. 2013. Adaptation-based resistance to siderophore-conjugated antibacterial agents by *Pseudomonas aeruginosa*. Antimicrob Agents Chemother 57:4197–4207.

Tortora ML, Diaz-Ricci JC, Pedraza RO. 2011. *Azospirillum brasilense* siderophores with antifungal activity against *Colletotrichum acutatum*. Arch Microbiol 193:275–286.

Tripathi A, Schofield MM, Chlipala GE, Schultz PJ, Yim I, Newmister SA, Nusca TD, Scaglione JB, Hanna PC, Tamayo-Castillo G, Sherman DH. 2014. Baulamycins A and B, broad-spectrum antibiotics identified as inhibitors of siderophore biosynthesis in *Staphylococcus aureus* and *Bacillus anthracis*. J Am Chem Soc 136:1579–1586.

Wasylenki LE, Anbar AD, Liermann LJ, Mathur R, Gordon GW, Brantley SL. 2007. Isotope fractionation during microbial metal uptake measured by MC-ICP-MS. J Anal At Spectrom 22:905–910.

Weber T, Bongaerts J, Evers S, Maurer K. 2010. New microorganisms, having at least one mutation in ferric uptake regulator (fur) gene for inhibiting the expression of the fur gene when compared to a second microorganism that does not have the mutation, useful for producing CNY siderophores. Patent No. DE102009000989-A1.

Wencewicz TA, Miller MJ. 2013. Biscatecholate-monohydroxamate mixed ligand siderophore-carbacephalosporin conjugates are selective sideromycin antibiotics that target *Acinetobacter baumannii*. J Med Chem 56:4044–4052.

Wencewicz TA, Moellmann U, Long TE, Miller MJ. 2009. Is drug release necessary for antimicrobial activity of siderophore-drug conjugates? Syntheses and biological studies of the naturally occurring salmycin "Trojan Horse" antibiotics and synthetic desferridanoxamine-antibiotic conjugates. Biometals 22:633–648.

Willemse-Erix DFM, Jachtenberg JW, Schut TB, van Leeuwen W, van Belkum A, Puppels G, Maquelin K. 2010. Towards Raman-based epidemiological typing of *Pseudomonas aeruginosa*. J Biophotonics 3:506–511.

Yang Y-L, Xu Y, Kersten RD, Liu W-T, Meehan MJ, Moore BS, Bandeira N, Dorrestein PC. 2011. Connecting chemotypes and phenotypes of cultured marine microbial assemblages by imaging mass spectrometry. Angew Chem Int Edit 50:5839–5842.

Ye L, Ballet S, Hildebrand F, Laus G, Guillemyn K, Raes J, Matthijs S, Martins J, Cornelis P. 2013. A combinatorial approach to the structure elucidation of a pyoverdine siderophore produced by a *Pseudomonas putida* isolate and the use of pyoverdine as a taxonomic marker for typing P-putida subspecies. Biometals 26:561–575.

Yin WB, Baccile JA, Bok JW, Chen YM, Keller NP, Schroeder FC. 2013. A nonribosomal peptide synthetase-derived Iron(III) complex from the pathogenic fungus *Aspergillus fumigatus*. J Am Chem Soc 135:2064–2067.